Inorg. Chem. **2002**, *41*, 4444–4452

Synthesis and Ligand-Based Mixed Valency of *cis*- and *trans*-$Cr^{III}(X_4SQ)(X_4Cat)(L)_n$ (X = Cl and Br, *n* = 1 or 2) Complexes: Effects of Solvent Media on Intramolecular Charge Distribution and Ligand Dissociation of $Cr^{III}(X_4SQ)_3$

Ho-Chol Chang, Katsunori Mochizuki, and Susumu Kitagawa*

Department of Synthetic Chemistry and Biological Chemistry, Graduate School of Engineering, Kyoto University, Sakyo-ku, Kyoto 606-8501, Japan

Received April 10, 2002

The treatment of $Cr^{III}(X_4SQ)_3$ (SQ = *o*-semiquinonate; X = Cl and Br) with acetonitrile affords *trans*-$Cr^{III}(X_4SQ)(X_4Cat)(CH_3CN)_2$ (X = Cl (**1**) and Br (**2**)). In the presence of 2,2′-bipyridine (bpy) or 3,4,7,8-tetramethyl-1,10-phenanthrene (tmphen), the reaction affords $Cr^{III}(X_4SQ)(X_4Cat)(bpy)\cdot n CH_3CN$ (X = Cl, *n* = 1 (**3**); X = Br, *n* = 0.5 (**4**)) or $Cr^{III}(X_4SQ)(X_4Cat)(tmphen)$ (X = Cl (**5**) and Br (**6**)), respectively. All of the complexes show a ligand-based mixed-valence (LBMV) state with SQ and Cat ligands. The LBMV state was confirmed by the presence of the interligand intervalence charge-transfer band. Spectroscopic studies in several solvent media demonstrate that the ligand dissociation included in the conversion of $Cr^{III}(X_4SQ)_3$ to **1**–**6** occurs only in solvents with relatively high polarity. On the basis of these results, the effects of solvent media were examined and an equilibrium, $Cr^{III}(X_4SQ)_3 \leftrightarrow Cr^{III}(X_4BQ)(X_4SQ)(X_4Cat)$ (BQ = *o*-benzoquinone), is proposed by assuming an interligand electron transfer induced by solvent polarity.

Introduction

A metal complex containing noninnocent ligands serves as a useful module for novel supramolecular assemblies with intriguing physical and/or chemical properties based on valence and spin states. This could be exemplified by a family of *o*-quinone complexes that provide unique oxidation and spin states irrespective of their simple constituent, $C_6O_2X_4$ (X = H, halogen atom, etc.).[1] The degree of freedom of their electronic states, for instance, is ascribed to the versatile redox forms of *o*-benzoquinone (BQ), *o*-semiquinonate ($SQ^{\bullet -}$), and catecholate (Cat^{2-}).

Recent studies have demonstrated that the delicate balance of the distribution of the charge and the spin over a whole molecule gives rise to "valence tautomerism".[1a,b] The tautomerism has been observed for several transition metal complexes, in particular, manganese and cobalt complexes with two *o*-quinone ligands that chelate to the metal ions, $M(Q)_2(N\text{-}N)$ (Q = *o*-quinonate, N-N = nitrogen-donor ancillary ligand such as 2,2′-bipyridine). For the cobalt complexes, the tautomerism occurs between low-spin Co^{III} (left) and high-spin Co^{II} (right) isomers with mixed and homovalent ligands, respectively (eq 1).[1b,2] On the other hand, the manganese complexes show an equilibrium (eq 2) including three valence tautomers.[3] In the equilibria 1 and 2 the metal ions and the ligands simultaneously change their oxidation states in each step. The change in valence results from the combined redox activity of the metal ion and the *o*-quinone ligands, in other words, comes from the degree of freedom in the electronic state of the metal (M)/ligand (L) pair (M−L mechanism).

$$ls\text{-}Co^{III}(SQ)(Cat)(N\text{-}N) \leftrightarrow hs\text{-}Co^{II}(SQ)_2(N\text{-}N) \quad (1)$$

$$Mn^{IV}(Cat)_2(N\text{-}N) \leftrightarrow hs\text{-}Mn^{III}(SQ)(Cat)(N\text{-}N) \leftrightarrow hs\text{-}Mn^{II}(SQ)_2(N\text{-}N) \quad (2)$$

In contrast with the M−L mechanism, when the ligands act as dominant active sites against an inner and/or an outer

* Author to whom correspondence should be addressed. E-mail: kitagawa@sbchem.kyoto-u.ac.jp.

(1) (a) Pierpont, C. G.; Lange, C. W. *Prog. Inorg. Chem.* **1994**, *41*, 331. (b) Pierpont, C. G. *Coord. Chem. Rev.* **2001**, *216*−*217*, 99. (c) Pierpont, C. G. *Coord. Chem. Rev.* **2001**, *219*−*221*, 415.

(2) (a) Jung, O.-S.; Pierpont, C. G. *J. Am. Chem. Soc.* **1994**, *116*, 2229. (b) Adams, D. M.; Noodleman, L.; Hendrickson, D. N. *Inorg. Chem.* **1997**, *36*, 3966.

10.1021/ic025643p CCC: $22.00
Published on Web 07/17/2002

sphere electron-transfer processes, we could expect another mechanism, viz., the L−L mechanism, which is realized by a combination of a redox *inert* metal ion and *o*-quinone ligands.[4] Chromium(III) complexes, $Cr^{III}(X_4SQ)_3$ (X = Cl and Br),[5] demonstrate good examples of the stepwise chemical oxidation/reduction processes occurring on the ligand moieties as shown in eq 3. Among these seven-membered redox isomers, ligand-based mixed-valence (LBMV) redox isomers, $[Cr^{III}(X_4SQ)_{3-n}(X_4Cat)_n]^{n-}$ (n = 1−2), have been isolated by stepwise one- and two-electron reduction.[6]

$$[Cr^{III}(BQ)_3]^{3+} \leftrightarrow [Cr^{III}(BQ)_2(SQ)]^{2+} \leftrightarrow [Cr^{III}(BQ)(SQ)_2]^{+} \leftrightarrow Cr^{III}(SQ)_3 \leftrightarrow [Cr^{III}(SQ)_2(Cat)]^{-} \leftrightarrow [Cr^{III}(SQ)(Cat)_2]^{2-} \leftrightarrow [Cr^{III}(Cat)_3]^{3-} \quad (3)$$

To activate and to control the L−L mechanism, particular attention needs to be paid to the effects of the solvent media. Previous studies have demonstrated that the ligand-based redox reactions smoothly proceed in a *nonpolar solvent* such as dichloromethane and carbon disulfide. The reactions proceed in support of the kinetic inertness of the Cr(III) ion against the ligand exchange reaction in the nonpolar solvents. Pierpont et al. have reported that the ligand exchange reaction of $Cr^{III}(SQ)_3$ with 2,2′-bipyridine (bpy) is hardly discernible in a nonpolar solvent.[7] On the other hand, once $Cr^{III}(SQ)_3$ is chemically oxidized to the $[Cr^{III}(BQ)(SQ)_2]^+$ cation (eq 3), drastic enhancement of the reaction rate is achieved to give $Cr^{III}(SQ)(Cat)(bpy)$. The coordination ability of the BQ ligand is much weaker than the coordination abilities of $SQ^{\bullet-}$ and Cat^{2-}; therefore, the ligand exchange reaction readily occurs by bpy. In this context, the unique charge distribution over the three ligands in $Cr^{III}(SQ)_3$ provides structural rigidity, supporting successfully the L−L mechanism on the *o*-quinone ligands.

In this manuscript, we first demonstrate that $Cr^{III}(X_4SQ)_3$ only undergoes a rapid ligand exchange reaction with the nitrogen-donor chelate reagents or solvent molecules in *polar solvent*. The reaction was carried out without any oxidizing processes to give *cis*/*trans*-$Cr^{III}(X_4SQ)(X_4Cat)(L)_n$ LBMV complexes. On the basis of these reactions, we discuss effects of solvent media and their polarity on the intramolecular charge distribution together with the ligand dissociation of $Cr^{III}(X_4SQ)_3$. To date only one tris(*o*-quinone) complex, Mn^{III}(3,6-DTBSQ)$_3$, is known to show a temperature-dependent valence tautomeric equilibrium, $Mn^{III}(SQ)_3 \leftrightarrow Mn^{IV}(SQ)_2(Cat)$, based on the M−L mechanism.[3a] In contrast, the charge distribution in $Cr^{III}(X_4SQ)_3$ could be affected by the solvent media, where intramolecular electron transfer, the L−L mechanism, occurs between the redox-active ligand moieties through the redox inert chromium(III) ion.

Experimental Section

Materials. All chemicals were reagent grade. 3,4,7,8-Tetramethyl-1,10-phenanthroline was purchased from Aldrich and 2,2′-bipyridine from Tokyo Kasei Co., Ltd. Complexes $Cr^{III}(X_4SQ)_3 \cdot 4C_6H_6$ were synthesized by the procedure described in the literature.[6a] All of the reagents and solvents were used without special purification.

Preparation of the Complexes. ***trans*-$Cr^{III}(Cl_4SQ)(Cl_4Cat)(CH_3CN)_2$ (1).** A 350 mL carbon disulfide solution containing $Cr^{III}(Cl_4SQ)_3 \cdot 4C_6H_6$ (980 mg, 0.889 mmol) was added to 150 mL of acetonitrile and stirred for 1 day. The resulting suspension was filtered, and the obtained powder was washed several times with carbon disulfide and then dried in a vacuum (481 mg, 86%). A single crystal of **1** was grown from a layered solution of carbon disulfide containing $Cr^{III}(Cl_4SQ)_3$ and acetonitrile. Found: C, 30.46; H, 1.15; N, 4.46. Required for $C_{14}H_6Cl_8CrN_2O_4$: C, 30.71; H, 0.97; N, 4.48. IR (KBr): 2325w (ν_{CN}), 2297w (ν_{CN}), 1517w, 1472w, 1439m, 1407w, 1361w, 1314s, 1259w, 1238w, 1155s, 1037m, 981s, 952m, 813w, 794s, 691m, 669w, 585w, 549w, 524m, 444s, and 399s cm^{-1}.

***trans*-$Cr^{III}(Br_4SQ)(Br_4Cat)(CH_3CN)_2$ (2).** A 1000 mL carbon disulfide solution containing $Cr^{III}(Br_4SQ)_3 \cdot 4C_6H_6$ (3.50 g, 2.14 mmol) was added to 430 mL of acetonitrile and stirred for 1 day. The resulting suspension was filtered, and the obtained powder was washed with carbon disulfide several times and then dried in a vacuum (1.20 g, 57%). Found: C, 19.60; H, 0.76; N, 2.84. Required for $C_{14}H_6Br_8CrN_2O_4$: C, 19.58; H, 0.62; N, 2.85. IR (KBr): 2322w (ν_{CN}), 2293w (ν_{CN}), 1471w, 1464w, 1456w, 1429w, 1273s, 1199m, 1139s, 1037m, 938s, 756m, 746w, 702s, 654w, 628w, 614w, 596w, 566w, 533w, 518w, 496w, 478w, 423s, 430s, 421s, 402s, and 394s cm^{-1}.

$Cr^{III}(Cl_4SQ)(Cl_4Cat)(bpy)\cdot CH_3CN$ (3). A 130 mL acetonitrile suspension containing $Cr^{III}(Cl_4SQ)_3 \cdot 4C_6H_6$ (98 mg, 0.090 mmol) was heated under air, and then a 20 mL acetonitrile solution containing bpy (14 mg, 0.090 mmol) was added. The brownish violet suspension became reddish violet in few minutes. The suspension was filtered, and the filtrate was allowed to stand for 5 days. The violet crystals grown from the filtrate were collected by filtration, washed with acetonitrile several times, and then dried in a vacuum (27 mg, 41%). Found: C, 39.00; H, 1.61; N, 6.24. Required for $C_{24}H_{11}Cl_8CrN_3O_4$: C, 38.90; H, 1.50; N, 5.67. IR (KBr): 1571w, 1566w, 1495m, 1471s, 1430s, 1376m, 1313m, 1272m, 1247s, 1216s, 1170w, 1157w, 1131w, 1104w, 1090w, 1069w, 1059w, 1045w, 1034w, 978s, 885w, 813w, 791s, 766s, 731m, 711w, 691m, 663w, 651w, 630w, 611w, 592m, 581m, 550m, 535w, 514w, 460w, 444w, and 423w cm^{-1}.

$Cr^{III}(Br_4SQ)(Br_4Cat)(bpy)\cdot{}^1/_2CH_3CN$ (4). A hot 60 mL acetonitrile suspension containing $Cr^{III}(Br_4SQ)_3 \cdot 4C_6H_6$ (334 mg, 0.204 mmol) was treated in a 10 mL acetonitrile solution containing bpy (32 mg, 0.20 mmol) under air. The brownish violet suspension turned to violet in few minutes. The microcrystalline solid was collected by filtration, washed with acetonitrile several times, and then dried in a vacuum (157 mg, 72%). Found: C, 25.46; H, 0.94; N, 3.04. Required for $C_{23}H_{9.5}Br_8CrN_{2.5}O_4$: C, 25.67; H, 0.89; N, 3.25. IR (KBr): 1564w, 1494m, 1469m, 1445s, 1425s, 1349w, 1310m, 1283m, 1249s, 1208w, 1155s, 1124s, 1105s, 1081s, 1060s,

(3) (a) Attia, A. S.; Pierpont, C. G. *Inorg. Chem.* **1998**, *37*, 3051. (b) Attia, A. S.; Pierpont, C. G. *Inorg. Chem.* **1997**, *36*, 6184. (c) Attia, A. S.; Jung, O.-S.; Pierpont, C. G. *Inorg. Chim. Acta* **1994**, *226*, 91.
(4) Chaudhuri, P.; Hess, M.; Hildenbrand, K.; Bill, E.; Weyhermüller, T.; Wieghardt, K. *Inorg. Chem.* **1999**, *38*, 2781.
(5) (a) Pierpont, C. G.; Downs, H. H.; Rukavina, T. G. *J. Am. Chem. Soc.* **1974**, *96*, 5573. (b) Pierpont, C. G.; Downs, H. H. *J. Am. Chem. Soc.* **1976**, *98*, 4834.
(6) (a) Chang, H.-C.; Ishii, T.; Kondo, M.; Kitagawa, S. *J. Chem. Soc., Dalton Trans.* **1999**, 2467. (b) Chang, H.-C.; Miyasaka, H.; Kitagawa, S. *Inorg. Chem.* **2001**, *40*, 146. (c) Chang, H.-C.; Kitagawa, S. *Angew. Chem., Int. Ed.* **2002**, *41*, 130.
(7) Buchanan, R. M.; Claflin, J.; Pierpont, C. G. *Inorg. Chem.* **1983**, *22*, 2552.

1044s, 1035s, 1023s, 965s, 933s, 886m, 757s, 748s, 729m, 686m, 665m, 651m, 645m, 627m, 576w, 564w, 535w, 504w, 473w, 452m, 404m, and 397m cm^{-1}.

$Cr^{III}(Cl_4SQ)(Cl_4Cat)(tmphen)$ (5). The complex was synthesized by a procedure similar to that of **4** using $Cr^{III}(Cl_4SQ)_3 \cdot 4C_6H_6$ (221 mg, 0.2 mmol) and tmphen (48 mg, 0.20 mmol). Recrystallization from chloroform affords reddish violet single crystals (87 mg 56%). Found: C, 43.40; H, 2.45; N, 3.49. Required for $C_{28}H_{16}Cl_8CrN_2O_4$: C, 43.11; H, 2.07; N, 3.59. IR (KBr): 1532m, 1432m, 1402m, 1374w, 1306s, 1248m, 1101s, 1079s, 977s, 936w, 898m, 863w, 827w, 813w, 783s, 750w, 726w, 707w, 690w, 683w, 672w, 642w, 630w, 614w, 589m, 575w, 552w, 535w, 515w, 485w, 459w, 424w, and 404w cm^{-1}.

$Cr^{III}(Br_4SQ)(Br_4Cat)(tmphen)$ (6). A 65 mL acetonitrile suspension containing $Cr^{III}(Br_4SQ)_3 \cdot 4C_6H_6$ (378 mg, 0.231 mmol) was boiled under air, and then a 20 mL acetonitrile solution containing tmphen (56 mg, 0.24 mmol) was added. The brownish violet suspension turned to violet in few minutes. The suspension was filtered, and the filtrate was allowed to stand for 2 days. The powder obtained from the filtrate was collected by filtration, washed with acetonitrile several times, and then dried in a vacuum (147 mg, 55%). Found: C, 29.11; H, 1.49; N, 2.71. Required for $C_{28}H_{16}Br_8CrN_2O_4$: C, 29.61; H, 1.42; N, 2.47. IR (KBr): 1528m, 1469m, 1427m, 1398m, 1376m, 1308w, 1284m, 1267s, 1246m, 1232w, 1198w, 1114s, 933m, 896w, 871w, 812w, 752m, 727m, 722m, 700s, 660w, 623w, 597w, 569w, 556w, 531w, 495w, 434m, and 424m cm^{-1}.

Physical Measurements. Infrared spectra for KBr pellets were recorded on a Perkin-Elmer system 2000 FT-IR spectrometer over the range 350−7000 cm^{-1}, and absorption spectra on a Hitachi U-3500 spectrophotometer over the range 3130−33000 cm^{-1} at 296 K. Electrochemical measurements were carried out by a BAS CV-50W polarographic analyzer. A standard three-electrode system was used with glassy carbon working electrode, platinum-wire counter electrode, and $Ag/Ag^+/CH_3CN$ electrode as reference. Thermogravimetric analyses were made on a Rigaku Thermo Plus 2/TG8120 over the temperature range 295−772 K. Magnetic susceptibilities were recorded over the temperature range 1.9−350 K at 1 T with a superconducting quantum interference device (SQUID) susceptometer (Quantum Design, San Diego, CA) interfaced with a HP Vectra computer system. All of the values were corrected for diamagnetism that were calculated from Pascal's table.[8]

Crystallographic Data Collection and Refinement of Structures. All of the measurements were performed on a Rigaku mercury diffractometer with CCD two-dimensional detector with Mo Kα radiation employing a graphite monochromator at 296 K. The sizes of the unit cells were calculated from the reflections collected on the setting angles of seven frames by changing ω by 0.5° for each frame. Two different χ settings were used, and ω was changed by 0.5° per frame. Intensity data were collected in 480 frames with an ω scan width of 0.5° and exposure times 120, 70, and 180 s for **1**, **3**, and **5**, respectively. Empirical absorption correction using the program REQABA[9a] was performed for all of the data. All of the crystal data are summarized in Table 1. The structures were solved by direct methods[9b] and expanded using Fourier techniques.[9c] The final cycles of the full-matrix least-squares refinements were based on the observed reflections ($I > 3\sigma(I)$ for **1** and **3** and $I > 2\sigma(I)$ for **5**). All of the calculations were performed using the teXsan crystallographic software package of Molecular Structure Corporation.[9d]

(8) Kahn, O. Molecular Magnetism; VCH: New York, 1993.

Table 1. Crystallographic and Refinement Data for **1**, **3**, and **5**

	1	**3**	**5**
formula	$C_{16}H_6Cl_8N_2O_4Cr$	$C_{24}H_{11}Cl_8N_3O_4Cr$	$C_{16}H_{16}Cl_8N_2O_4Cr$
fw	625.85	740.99	780.07
color	reddish violet	reddish violet	reddish violet
cryst syst	triclinic	triclinic	monoclinic
space group	$P\bar{1}$	$P\bar{1}$	$C2/c$
a, Å	5.9174(8)	8.629(2)	16.128(7)
b, Å	9.4798(8)	13.739(2)	26.148(5)
c, Å	10.672(2)	14.714(3)	8.5648(9)
α, deg	109.517(5)	115.71(1)	90
β, deg	99.967(3)	95.706(3)	102.944(2)
γ, deg	92.822(2)	92.154(4)	90
Z	1	2	4
V, Å^3	522.0(1)	1557.6(6)	3520(1)
ρ_{calcd}, g/cm^3	1.882	1.580	1.472
μ, cm^{-1}	15.13	10.87	9.66
T, K	296	296	296
λ (Mo Kα), Å	0.71069	0.71069	0.71069
no. of reflns	2991	3207	1334[a]
no. of params	154	361	195
refln/param ratio	19.4	8.88	6.9
GOF	1.678	1.248	1.405
R_{int}	0.015	0.028	0.038
R, R_w[b]	0.042, 0.084	0.053, 0.072	0.074, 0.089

[a] $I > 2.0\sigma(I)$. [b] $R = \sum||F_o| - |F_c||/\sum|F_o|$, $R_w = [\sum w(|F_o| - |F_c|)^2/\sum w|F_o|^2]^{1/2}$.

Results and Discussion

Molecular Structures and Crystal Packing Structures. Figure 1 shows ORTEP drawings of **1**, **3**, and **5** with an atom-numbering scheme. Table 2 lists selected average bond distances and angles of the complexes. Each chromium ion has a distorted octahedral coordination environment involving four oxygen atoms from the two *o*-quinone ligands and two nitrogen atoms from the acetonitriles (**1**), bpy (**3**), and tmphen (**5**). The acetonitrile ligands in **1** coordinate to the chromium ion in a trans fashion, allowing two *o*-quinone ligands to sit coplanarly. The Cr−O bond distances are found to be 1.929(3) and 1.935(3) Å for Cr(1)−O(1) and Cr(1)−O(2) bonds, respectively, and the average distance, 1.932(3) Å, is similar to those of the series of $[Cr^{III}(X_4SQ)_{3-n}(X_4Cat)_n]^{n-}$ isomers,[6a,b] indicating the trivalent nature of the chromium atom. As a complex of Cr(III), a formal combination of a X_4SQ and X_4Cat can be suggested for charge distribution on the quinone ligands. In many cases the crystallographic symmetry, however, averages dissimilar ligands, giving bond distances for the C−O bonds that are intermediate between SQ and Cat values.[3] The chromium atom of **1** is, in fact, on a special position that averages the structural features of the two *o*-quinone ligands. The observed C−O bond distance for **1** is 1.310(5) Å, which is intermediate between 1.28 and 1.34 Å for typical SQ and Cat forms, respectively.

On the other hand, complex **3** has two crystallographically independent *o*-quinone ligands, **I** and **II**, where the dihedral

(9) (a) Jacobson, R. A. *REQABA Empirical Absorption Correction Version 1.1−03101998*; Molecular Structure Corp.: The Woodlands, TX, 1996−1998. (b) Altomare, A.; Burla, M. C.; Camalli, M.; Cascarano, M.; Giacovazzo, C.; Guagliardi, A.; Pilidori, G. *J. Appl. Crystallogr.* **1994**, *27*, 435. (c) Beurskens, P. T.; Admiraal, G.; Beurskens, G.; Bosman, W. P.; de Gelder, R.; Israel, R.; Smits, J. M. M. *The DIRDIF-94 program system*; Technical Report of the Crystallography Laboratory; University of Nijmegen: Nijmegen, The Netherlands, 1994. (d) *teXsan, Crystal Structure Analysis Package*; Molecular Structure Corporation: The Woodlands, TX, 1985, 1992.

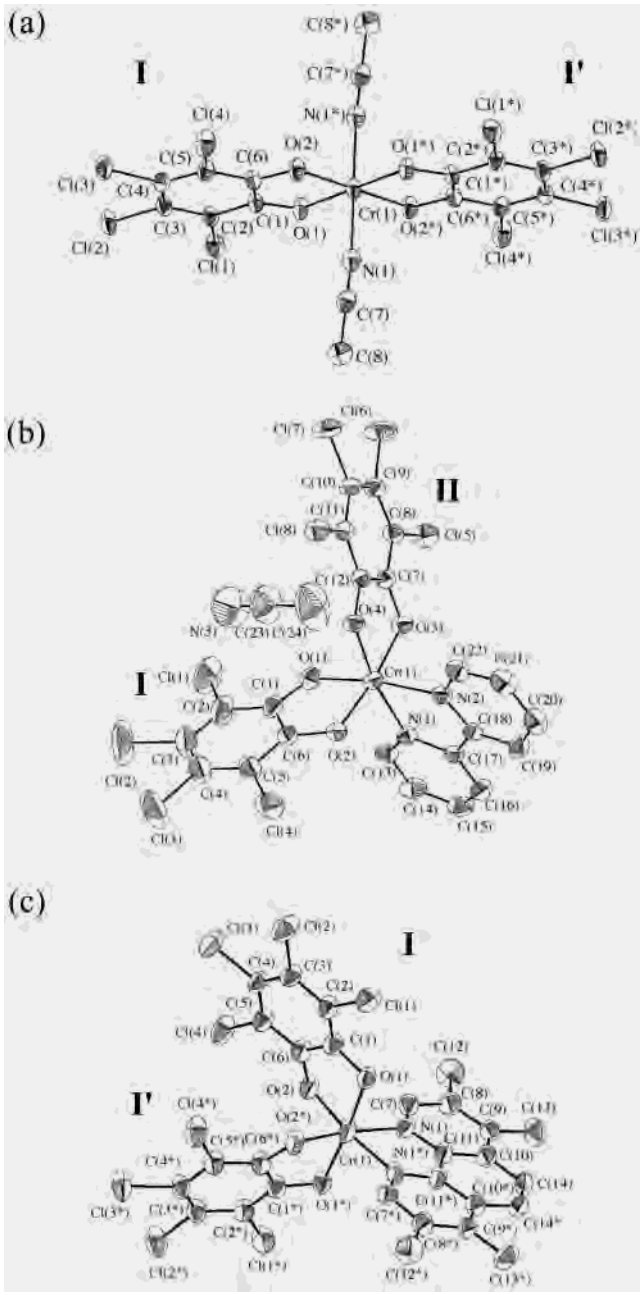

Figure 1. ORTEP drawings of (a) **1**, (b) **3**, and (c) **5** with hydrogen atoms omitted (showing 30% isotropic thermal ellipsoids). Crystallographically independent ligands are designated **I** and **II**. The chromium atoms of **1** and **5** have centroids coincident with crystallographic symmetry.

angle between two ligands defined by $C_6O_2Cl_4$ planes is 98.8(1)°. The C−O bond distances of 1.326(8) and 1.344(8) Å for ligand **I** are slightly longer than those of 1.301(6) and 1.314(7) Å for ligand **II**. These structural differences imply a localized mixed-valence state for the two independent ligands. In general, the ligand bite angle of the SQ ligand is typically 2° smaller than that of the Cat ligand.[10] This tendency is also observed for two independent ligands, where the O(1)−Cr(1)−O(2) angle of ligand **I** (Cat) is 84.4(2)°, larger than the 82.9(2)° angle of ligand **II** (SQ).

(10) Sofen, S. R.; Ware, D. C.; Cooper, S. R.; Raymond, K. N. *Inorg. Chem.* **1979**, *18*, 234.

Table 2. Selected Average Bond Distances (Å) and Angles (deg) of **1**, **3**, and **5**

		1	**3**			**5**
	L		trans[a]	cis[b]	av	
Cr−O (Å)	**I**	1.934	1.911(4)	1.945(4)	1.939	1.912
	II		1.943(4)	1.955(4)	1.949	
av		1.934			1.939	1.912
C−O (Å)	**I**	1.311	1.327(8)	1.335(7)	1.331	1.34
	II		1.312(6)	1.308(6)	1.310	
av		1.311			1.321	1.34
Cr−N (Å)		2.040(4)			2.062	2.060(9)
O−Cr−O (deg)	**I**	83.68(10)		84.4(2)		85.1(3)
	II			82.9(1)		
av		83.68(10)		83.7		85.1(3)
N−Cr−N (deg)		180.0(0)			78.5(2)	78.3(5)
N(1)−Cr(1)−O(1)−C(1) (deg)				99.5(1)		119.7(8)
N(1)−Cr(1)−O(2)−C(6) (deg)				−99.2(4)		−117.1(7)
N(2)−Cr(1)−O(1)−C(1) (deg)				70(1)		
N(2)−Cr(1)−O(2)−C(6) (deg)				−177.8(4)		
Cr(1)−O(1)−C(1)−C(6) (deg)				−5.4(7)		−17(1)
Cr(1)−O(2)−C(6)−C(1) (deg)				4.7(6)		21(1)
Cr(1)−O(3)−C(7)−C(12) (deg)				11.9(6)		
Cr(1)−O(4)−C(12)−C(7) (deg)				−8.0(6)		

[a] Oxygen atom trans to the nitrogen atom. [b] Oxygen atom cis to the nitrogen atom.

In contrast to complex **3**, in the crystallographic symmetry of complex **5** the two different *o*-quinone ligands similar to the situation for complex **1** are unable to be distinguished. Interestingly, the most striking feature of complex **5** is the heavily bent geometry of the quinone ligands. The six-membered carbon ring plane of the ligand **I** forms a dihedral angle of 25.3° with its CrO_2 chelate plane. This angle is larger than 5.5° and 14.4° for ligands **I** and **II** of complex **3**, respectively. The observed bend could be attributed to the difference of the crystal packing structures of **3** and **5**. As shown in Figure 2a the main intermolecular interaction in **3** is found for the overlap of adjacent bpy ligands with an interplanar separation of 3.505(8) Å. The ligands **I** and **II** also form intermolecular stacking structures, **I**···**I**′ and **II**···**II**′, with the adjacent complex molecules; however, their overlaps seem to be quite small. On the other hand complex **5** forms two independent columns of complex molecules. The first column consists of a stack linked by overlapping six-membered rings of the adjacent quinone ligand **I**···**I**′ (Figure 2b) along the *ac*-direction with a mean interplanar separation of 3.56(2) Å. The interaction causes the distortion of the ligands from the ideal planar geometry so that each ligand bends to the direction of the column.[11] Another one-dimensional column of the complexes occurs from the overlapping of the adjacent tmphen ligands along the *c*-axis (Figure 2c). Each tmphen column links the *o*-quinone columns to form a three-dimensional assembled structure of the complexes in the crystal (Figure 2d).

Spectroscopic Properties. UV−Vis−NIR−IR Absorption Spectra. Infrared spectra (KBr) of all of the complexes are shown in Figure 3. Each spectrum is depicted by two characteristic absorption bands observed near 1450 cm^{-1} and a broad, strong band near 1100 cm^{-1}. Similar spectra have been observed for $[Cr^{III}(X_4SQ)_{3-n}(X_4Cat)_n]^{n-}$ (n = 1−2) redox isomers with three *o*-quinonate ligands in the LBMV state.[6a,b] By comparing the spectra, the bands at 1450 and

(11) Pierpont, C. G.; Buchanan, R. M. *J. Am. Chem. Soc.* **1975**, *97*, 4912.

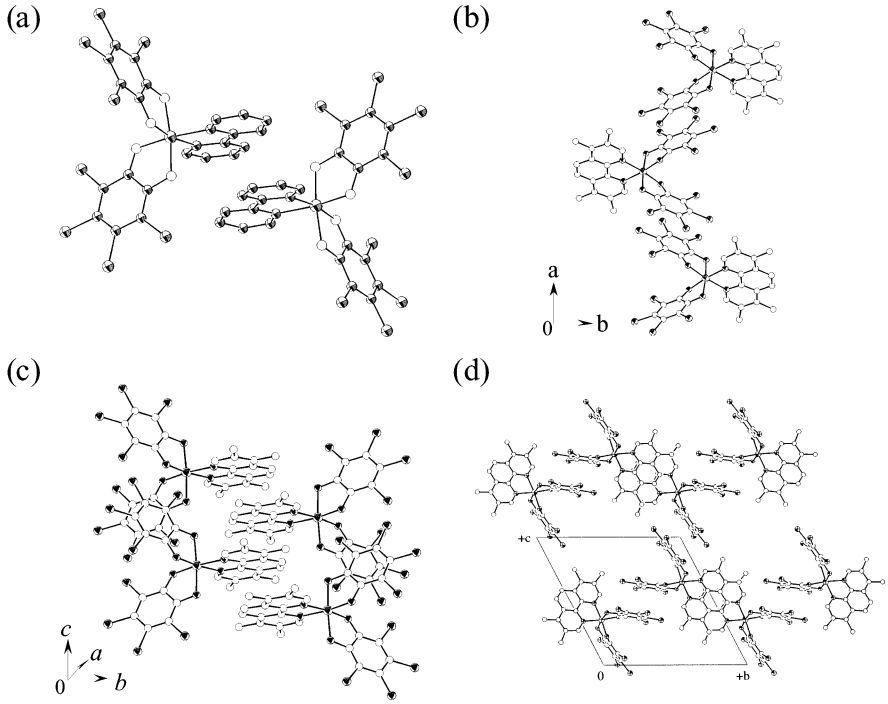

Figure 2. (a) View showing the pairing of complex **3** within unit cell. The separation between adjacent bpy ligands is 3.505(8) Å. (b) One-dimensional stacking structures of ligand **I** and **II** and (c) that of tmphen ligands in complex **5**. (d) Whole crystal packing diagram of **5** along the *a*-axis.

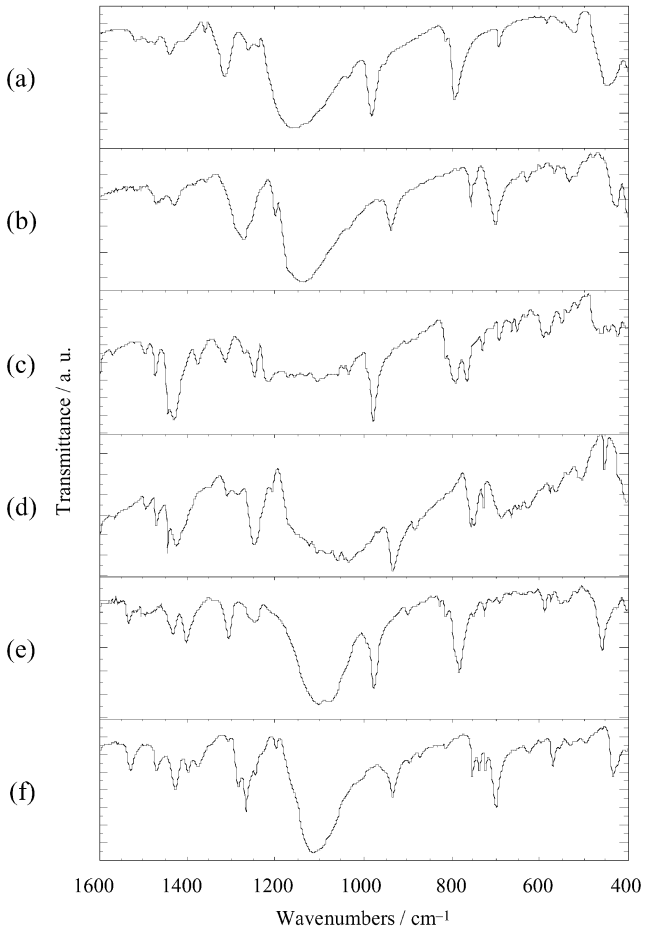

Figure 3. FT-IR spectra (KBr pellets) of complexes (a) **1**, (b) **2**, (c) **3**, (d) **4**, (e) **5**, and (f) **6**.

1100 cm^{-1} are assigned to the vibration modes characteristic for $SQ^{\bullet-}$ and Cat^{2-}, respectively. The data clearly demonstrates the LBMV state of **1**−**6**, although complexes **1** and **5** possess crystallographic ambiguity for distinction of the SQ and Cat ligands due to their crystallographic symmetry.

Table 3. Absorption Spectral Parameters for Complexes **1**−**6** in Solution

	$\nu_{max} \times 10^{-3}/cm^{-1}$ ($\epsilon_{max} \times 10^{-3}$ M^{-1} cm^{-1})
1[a]	5.08 (3.47), 7.41 (sh, 1.15), 8.47 (0.789), 11.0 (1.54), 13.6 (1.98), 15.9 (0.824), 19.0 (4.31), 24.8 (2.32)
2[a]	5.05 (4.26), 7.46 (sh, 1.35), 8.38 (0.948), 10.9 (1.61), 13.4 (2.16), 16.0 (0.808), 19.0 (0.507), 24.2 (2.58)
3[b]	4.32 (2.50), 11.2 (2.42), 12.7 (2.52), 14.0 (sh, 1.95), 15.6 (1.72), 18.1 (6.50), 21.6 (sh, 2.74), 24.8 (sh, 3.07), 32.9
4[b]	3.77, 11.2 (2.04), 12.6 (2.26), 13.9 (1.62), 15.7 (1.47), 18.1 (5.28), 21.4 (2.16), 23.9 (2.43), 33.2 (16.0)
5[b]	4.31 (2.12), 11.2 (2.34), 12.8 (2.47), 14.1 (sh, 1.51), 15.8 (1.41), 18.3 (5.96), 21.3 (2.68), 24.9 (2.95)
6[b]	11.1 (2.27), 12.6 (3.07), 14.5 (sh, 1.51), 15.9 (1.66), 18.2 (6.91), 21.4 (3.05), 24.0 (3.50)

[a] Measured in 1,2-dimethoxyethane. [b] Measured in dichloromethane.

Figure 4 shows UV−vis−NIR−IR absorption spectra of the complexes measured in solution (solid lines; 1,2-dimethoxyethane (**1**, **2**) and dichloromethane (**3**−**6**)) and on KBr pellets (dashed lines). The observed peak maxima are summarized in Tables 3 (solution) and 4 (solid). In the UV−visible region, all of the complexes commonly show several intense absorption bands. For the spectra in solution the bands near 14000 and 21000 cm^{-1} observed for **3**−**6** could be assigned to electronic transitions related to the nitrogen ancillary ligands, bpy and tmphen, because of the absence of the corresponding bands in **1** and **2**. The strongest electronic transition is commonly observed around 19000 cm^{-1} for all of the complexes, where the absorption energies of the bands for **1** and **2** are higher by 250 cm^{-1} than those of **3**−**6**. These bands have been observed in the complexes containing Cr^{III}-SQ moieties and, thus, are useful for chro-

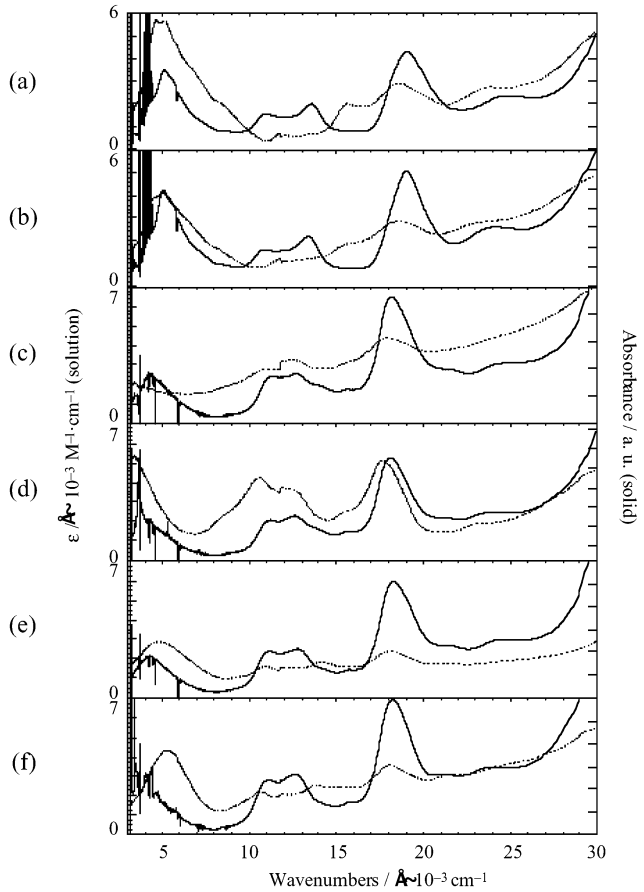

Figure 4. Electronic absorption spectra (solid lines) of (a) **1**, (b) **2**, (c) **3**, (d) **4**, (e) **5**, and (f) **6** in 1,2-dimethoxyethane (**1** and **2**) and dichloromethane (**3**−**6**) at 296 K. The dotted lines show electronic absorption spectra of the complexes measured on KBr pellets at 296 K. The discontinuity near 12000 cm^{-1} is an instrumental artifact due to a detector change in the spectrometer.

Table 4. Absorption Spectral Parameters for Complexes **1**−**6** Measured on KBr Pellets

	$\nu_{max} \times 10^{-3}/cm^{-1}$
1	4.62, 5.10, 5.90 (sh), 6.60 (sh), 8.20 (sh), 12.1, 13.5 (sh), 15.6, 18.6, 23.9
2	4.50 (sh), 5.00, 5.70 (sh), 6.45 (sh), 8.00 (sh), 12.0, 13.4 (sh), 15.6 (sh), 18.6, 23.5 (sh)
3	3.43, 4.00 (sh), 5.10 (sh), 5.80 (sh), 8.50 (sh), 11.1, 12.5, 15.3 (sh), 18.0, 24.0 (sh)
4	3.42, 4.20 (sh), 5.10 (sh), 8.40 (sh), 10.5, 12.2 (sh), 15.7 (sh), 17.6, 23.8
5	4.35 (sh), 4.73, 9.40 (sh), 10.9, 12.0 (sh), 14.2, 15.3, 18.1, 21.4, 25.0 (sh)
6	4.40 (sh), 5.22, 9.20 (sh), 9.90 (sh), 10.6, 12.0 (sh), 13.8, 14.6, 15.4, 18.9, 21.7, 25.0 (sh)

mophore identification.[12] The most prominent spectral features of spectra shown in the figures are the broad, intense absorption bands, with several overtone vibrational transitions, that appear in 3000−8000 cm^{-1} in each complex. Such low-energy electronic transitions have been observed in the series of tris-type $[Cr^{III}(X_4SQ)_{3-n}(X_4Cat)_n]^{n-}$ (n = 1, 2) LBMV isomers.[6] The bands have been assigned to interligand intervalence CT (IVCT) transitions of π^*(SQ) ← π^*(Cat),[2b] indicating the presence of the $SQ^{\bullet-}$ and Cat^{2-} ligands in **1**−**6**.

(12) (a) Benelli, C.; Dei, A.; Gatteschi, D.; Pardi, L. *Inorg. Chem.* **1989**, *28*, 1476. (b) Wheeler, D. E.; McCusker, J. K. *Inorg. Chem.* **1998**, *37*, 2296.

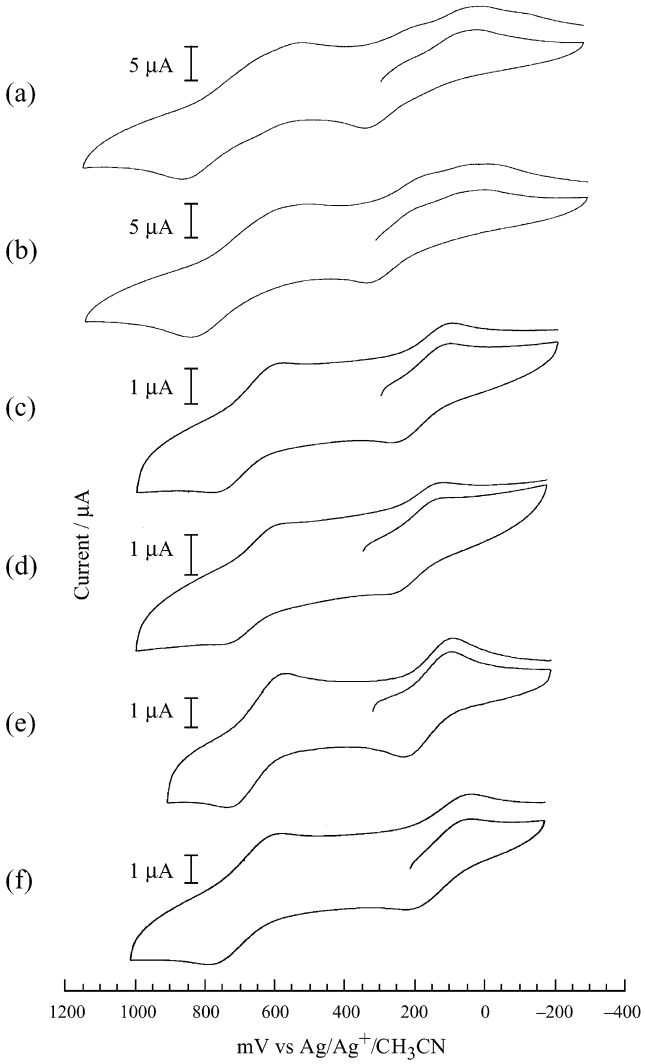

Figure 5. Cyclic voltammograms of complexes (a) **1**, (b) **2**, (c) **3**, (d) **4**, (e) **5**, and (f) **6** measured in 1,2-dimethoxyethane (**1** and **2**) and dichloromethane (**3**−**6**) at 296 K.

The intensities of the IVCT bands for complexes **1** and **2**, which contain two quinone ligands in a plane, show higher absorption intensities compared with those of **3**−**6**. In the solid state (KBr) all of the complexes show similar absorption spectra with slight blue or red shifts at each absorption maximum as shown in Figure 4 (dotted lines). The presence of the IVCT bands indicates that in the solid state all of the complexes possess the LBMV state.

Electrochemical Properties. Because of the redox-active nature of the ligand moieties, ligand-based electrochemical activity would be expected for the present complexes. The electrochemical properties of the complexes were studied in 1,2-dimethoxyethane and dichloromethane solution for **1** and **2** and **3**−**6**, respectively. The results are given in Figure 5 and Table 5. All of the complexes commonly undergo quasi-reversible one-electron oxidation and reduction near 630 and 170 mV vs $Ag/Ag^+/CH_3CN$, respectively. Because the chromium ion retains a trivalent state in this potential region, the electrochemical processes correspond to one-electron oxidation and reduction of the ligand moieties, respectively, as shown in eq 4.

Table 5. Electrochemical Data for Complexes **1**−**6**

	potential (mV vs $Ag/Ag^+/CH_3CN$)[a]												
			+1/0				0/−1						
	E_{ox2}	E_{ox1}	E_{ox}	E_{red}	Δ[d]	$E_{1/2}$	E_{ox}	E_{red}	Δ[d]	$E_{1/2}$	$\Delta E_{1/2}$[e]	E_{red1}	E_{red2}
1[b]		1400	817	505	312	661	327	6	321	167	494	−1440	
2[b]		1370	826	493	333	660	333	−9	342	162	498	−1560	
3[c,f]	1860		778	575	203	677	265	107	158	186	491		−1720
4[c]	1860		730	550	190	640	276	103	173	190	450	−1150	
5[c]	1170	1540	718	551	167	635	230	83	147	157	478	−1410	
6[c]	1730	1540	707	537	170	622	229	77	152	153	467	−1550	

[a] Conditions: scan rate 100 mV/s, N_2, 296 K. [b] Measured in 1,2-dimethoxyethane. [c] Measured in dichloromethane. [d] Separation between E_{ox} and E_{red}. [e] Separation between $E_{1/2}(+1/0) - E_{1/2}(0/-1)$. [f] Reference 7.

$$[Cr^{III}(X_4SQ)_2(L)_n]^+ \leftrightarrow [Cr^{III}(X_4SQ)(X_4Cat)(L)_n]^0 \leftrightarrow [Cr^{III}(X_4Cat)_2(L)_n]^- \quad (4)$$

1−**6**

The one-electron oxidation would provide a cationic $[Cr^{III}(X_4SQ)_2(L)_n]^+$ species (left) with two SQ ligands, while the reduction affords an anionic $[Cr^{III}(X_4Cat)_2(L)_n]^-$ species (right) with two Cat ligands. These electrochemical properties are similar to those observed for $Cr^{III}(SQ)(Cat)(bpy)$ complexes, as reported by Pierpont et al.[7] The reduction potentials of complexes **3** and **4** are higher than those of **5** and **6**, reflecting the electron-donating effect of methyl groups of the tmphen ligand. Similarly, lower oxidation potentials are observed for complexes **3** and **4** compared with complexes **5** and **6**. The differences between the first oxidation and the reduction potentials are approximately 500 mV for all of the complexes, which is comparable to 390 mV observed for the mixed-valence Creutz−Taube ion, $[(NH_3)_5Ru(py)Ru(NH_3)_5]^{5+}$ (py = pyrazine).[13] All of the complexes show irreversible reduction waves at potentials lower than −1400 mV. The process would be attributable to the reduction of the Cr^{III} to the Cr^{II}. Finally, one (**1**−**4**) or two (**5**, **6**) irreversible oxidation waves are also found. From a comparison with the redox properties of $Cr^{III}(X_4SQ)_3$, the oxidation of SQ to BQ would be attributable to these redox process.[14] The irreversible electrochemical process is forced by the low coordination ability of the neutral BQ ligand.

Thermogravimetric Analyses. To examine the thermolabilities of the axially coordinated acetonitrile ligands of **1** and **2**, thermogravimetric (TG-DTA) measurements were carried out. The TG-DTA diagrams of both complexes are given in Figure 6. Rapid weight losses of 14.2% (**1**) and 9.0% (**2**) take place up to 520 K for the two complexes. The liberation of two acetonitrile ligands accounts for this weight loss in **1** (13.1%) and in **2** (8.4%) (eq 5). Above this temperature, the complexes gradually lost weight, which indicated thermal decomposition.

$$trans\text{-}Cr^{III}(X_4SQ)(X_4Cat)(CH_3CN)_2 \rightarrow [Cr^{III}(X_4SQ)(X_4Cat)] + 2CH_3CN \quad (5)$$

1, **2**

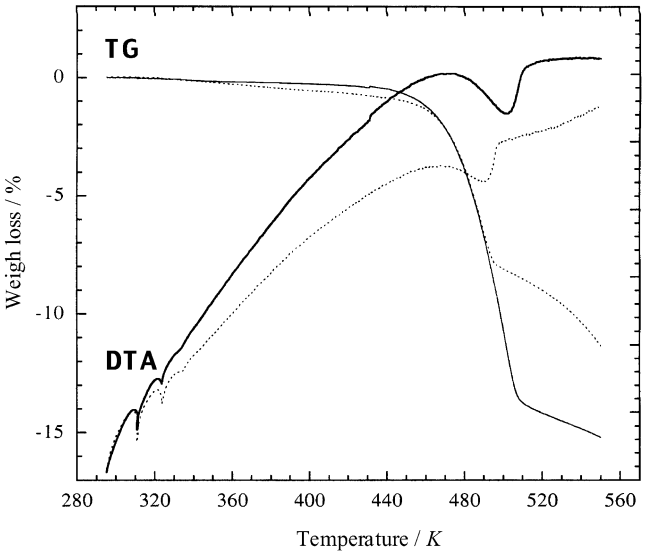

Figure 6. Thermogravimetric data for **1** (solid line) and **2** (dotted line).

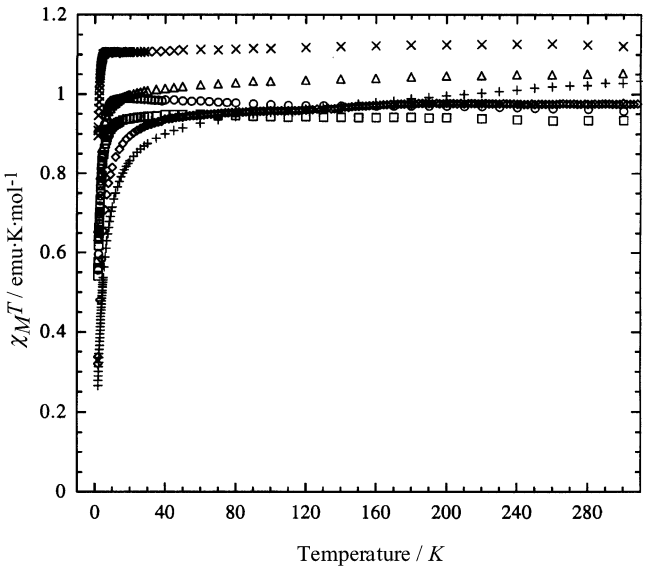

Figure 7. Plots of the temperature dependence of $\chi_M T$ for (a) **1** (○), (b) **2** (□), (c) **3** (◇), (d) **4** (×), (e) **5** (+), and (f) **6** (△) measured under a field of 1 T.

Temperature Dependence of Magnetic Susceptibilities. Figure 7 shows the temperature dependence of $\chi_M T$ for all of the complexes. At 300 K, the values are in the range 0.934−1.12 emu K mol^{-1}, close to the theoretical value of 1.00 emu K mol^{-1} expected for an $S = 1$ spin ($g = 2.00$).[8] The $S = 1$ ground state could be attributed to the intramo-

(13) (a) Creutz, C.; Taube, H. *J. Am. Chem. Soc.* **1973**, *95*, 1086. (b) Creutz, C. *Prog. Inorg. Chem.* **1983**, *30*, 1.
(14) Downs, H. H.; Buchanan, R. M.; Pierpont, C. G. *Inorg. Chem.* **1979**, *18*, 1736.

lecular antiferromagnetic interactions between an $S = {}^3/_2$ spin on the Cr(III) ion and an $S = {}^1/_2$ spin on the SQ ligand. No temperature dependence of $\chi_M T$ was observed in the region of 50−300 K for all of the complexes; therefore, it must be concluded that the coupling is strongly antiferromagnetic with a ground state $S = 1$ and no exited state thermally populated. These results are similar to those for the complex, $[Cr^{III}(tren)(3,6\text{-DTBSQ})](PF_6)_2$ (tren = tris(2-aminoethyl)-amine),[12b] containing the same spin components as the present complexes. The $\chi_M T$ values exhibit temperature independent behavior in the region of 50−300 K, while a rapid decrease was observed below 50 K. The decrease of $\chi_M T$ values is suggestive of intermolecular antiferromagnetic interactions between the neighboring complexes, which are attributable to the stacking interaction between the adjacent complex molecules.

Spectroscopic Studies of $Cr^{III}(X_4SQ)_3$ in Nonpolar and Polar Solvents. $Cr^{III}(X_4SQ)_3$ undergoes stepwise ligand-based reduction as shown in eq 3 to give seven-membered redox isomers including the LBMV complexes.[6,14] The one- and two-electron-reduced species are synthesized by charge-transfer reactions performed in nonpolar solvents such as dichloromethane and carbon disulfide. This is because $Cr^{III}(X_4SQ)_3$, with unique charge distribution over three ligands, is fairly stable in nonpolar solvents. On the other hand, the dissolution of $Cr^{III}(X_4SQ)_3$ in acetonitrile gives rise to a rapid formation of the dark purple solids of **1** and **2**. As reported by Pierpont et al., $Cr^{III}(SQ)_3$ shows poor ligand exchange reactivity in a nonpolar solvent owing to the kinetic inertness of the octahedral Cr^{III} (d^3).[7] On the other hand, once the one-electron-oxidized species of $[Cr^{III}(BQ)(SQ)_2]^+$ forms, a rapid ligand exchange with bpy occurs because of the weak coordination ability of the BQ ligand (eq 6). However, we found that in acetonitrile media the ligand exchange reaction proceeds without oxidation of the complex.

$$Cr^{III}(Cl_4SQ)_3 \xrightarrow{-e^-} [Cr^{III}(Cl_4BQ)(Cl_4SQ)_2]^+ \xrightarrow{bpy} Cr^{III}(Cl_4SQ)(Cl_4Cat)(bpy)\ (\mathbf{3}) + Cl_4BQ \qquad (6)$$

Since no chemical and spectroscopic studies of $Cr^{III}(SQ)_3$ in polar solvents have yet been reported,[15] the electronic absorption spectra of $Cr^{III}(Cl_4SQ)_3$ were determined in dichloromethane,[5a] carbon disulfide, cyclohexane, nitromethane, acetone, and benzonitrile to investigate the conversion of $Cr^{III}(X_4SQ)_3$ to **1**−**6**. As shown in Figure 8 (top), the spectra obtained for the solvents with a low dielectric constant (ϵ_r at 293 K), cyclohexane ($\epsilon_r = 2.02$), carbon disulfide ($\epsilon_r = 2.64$), and dichloromethane ($\epsilon_r = 9.02$), were found to be similar to each other. In these solvents, a strong absorption maxima (ϵ = ca. 20000 M^{-1} cm^{-1}) near 19000 cm^{-1} is found and no absorption bands lower than 7000 cm^{-1} in energy can be detected in the region. On the other hand, the dissolution of $Cr^{III}(Cl_4SQ)_3$ in polar solvents such as acetone ($\epsilon_r = 21.36$), benzonitrile ($\epsilon_r = 25.30$), or nitromethane ($\epsilon_r = 36.16$) causes a decrease of absorption intensities (ϵ = ca. 6000 M^{-1} cm^{-1}) of the bands near 19000 cm^{-1} and an

(15) Vlček, A., Jr. *Inorg. Chem.* **1986**, *25*, 522.

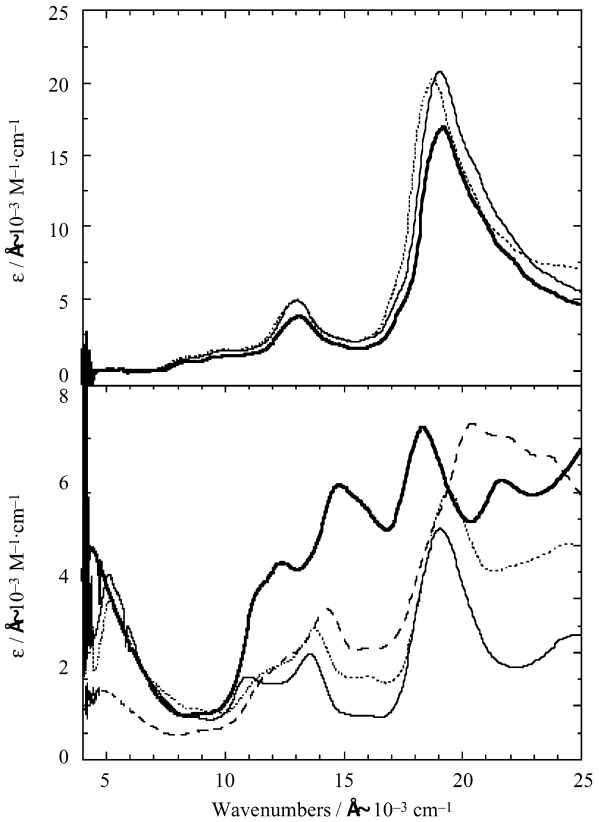

Figure 8. Electronic absorption spectra of $Cr^{III}(Cl_4SQ)_3$. Top: measured in dichloromethane (solid line), carbon disulfide (dotted line), and cyclohexane (bold line). Bottom: measured in acetone (dotted line), nitromethane (dashed line), and benzonitrile (bold line) together with the spectrum of complex **1** in 1,2-dimethoxyethane (solid line).

increase of the intensities in the region of 4000−8000 cm^{-1} as shown in Figure 8 (below). All of the spectra measured in the polar solvent are close to the spectrum of **1** measured in 1,2-dimethoxyethane, and drawn in Figure 8 (bottom) as a solid line, rather than to those of $Cr^{III}(Cl_4SQ)_3$ in the nonpolar solvents. The most prominent feature is the presence of the low-energy absorption band maxima near 4000 cm^{-1}, which is characteristic for the LBMV state (see above). A similar spectral change was observed in a dilute acetonitrile ($\epsilon_r = 36.00$) solution of $Cr^{III}(Cl_4SQ)_3$. These spectral features clearly indicate that the dissolution of $Cr^{III}(Cl_4SQ)_3$ in polar solvents causes the formation of LBMV species.

Since $Cr^{III}(X_4SQ)_3$ does not show spontaneous ligand dissociation or ligand substitution reaction in nonpolar media, the solvent polarity is significantly associated with the intramolecular charge distribution of the complexes. On the basis of the formation of **1**−**6** and observed spectral change by solvent polarity, a mechanism drawn in Scheme 1 would be one of the most possible mechanisms for the present system. Dissolution of $Cr^{III}(X_4SQ)_3$ in polar solvents would lead to a disproportionation of the charge on the ligand moieties, affording a tris-type LBMV species, $[Cr^{III}(X_4BQ)(X_4SQ)(X_4Cat)]$, with three different ligand forms. The LBMV species could be generated by an intramolecular interligand electron-transfer process in $Cr^{III}(X_4SQ)_3$. The observed spectra indicate that the equilibrium lies to the left in low-dielectric solvents, whereas in high-dielectric solvents

Scheme 1

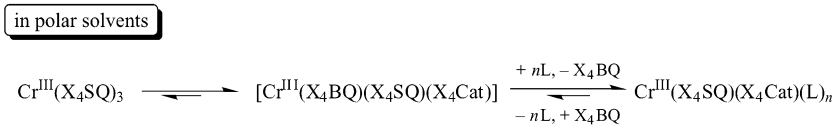

the equilibrium is driven to the right. Although the LBMV species could not be isolated or detected, it seems likely that the LMBV species is immediately followed by the dissociation of the X_4BQ ligand in the polar solvents because the X_4BQ ligand possesses the weakest coordination ability among the three redox isomers, BQ, $SQ^{\bullet -}$, and Cat^{2-}. In fact, the red crystals were isolated from the filtrate, and they show an infrared band at 1680 cm^{-1}, assigned to the C═O stretching mode of Cl_4BQ. If no chelate reagents such as bpy or tmphen are in the solution, the acetonitrile (solvent) molecules coordinate to the chromium(III) ion to form trans complexes **1** and **2**. While in the presence of the chelate reagents, cis-coordinated products should be generated.

The intramolecular electron transfers between the ligand and the metal ion occur by temperature, pressure, and light in the valence tautomeric cobalt and manganese complexes. Furthermore, Hendrickson et al. reported a solvent effect on charge distribution of $Fe(phenQ)_2(N\text{-}N)$ (phenQ = 9,10-phenathreneSQ/Cat) (eq 7),[16]

$$Fe^{II}(phenSQ)_2(N\text{-}N) \leftrightarrow Fe^{III}(phenSQ)(phenCat)(N\text{-}N) \quad (7)$$

where the equilibrium lies to the left in a high-dielectric solvent, and where in low-dielectric solvent the equilibrium is shifted to the right to give the LBMV tautomer. This tendency would be changed in the present system, where the high-dielectric solvent medium promotes the disproportionation of the charge over the three ligands. The difference between these two systems could be attributable to the difference of the metal ions used. Namely, in iron complexes, both metal ions and ligands can change their valence states (M−L mechanism), while with chromium complexes only the ligands could change their valence states (L−L mechanism), due to the thermodynamic stability of the chromium(III) ion. As shown in Scheme 1, we believe that in the solvent media with relatively high dielectric constants the homoleptic tautomer isomerizes rapidly to the tris-type LBMV species through the intramolecular interligand electron-transfer process. The LBMV species readily lose the X_4BQ ligand, followed by a ligand exchange reaction by the solvent molecules or the chelate reagents to give complexes **1**−**6**.

(16) Lynch, M. W.; Valentine, M.; Hendrickson, D. N. *J. Am. Chem. Soc.* **1982**, *104*, 6982.

Conclusion

In this work, we reported the synthesis of novel LBMV chromium complexes with two *o*-quinonate ligands, based on the internal charge distribution of $Cr^{III}(X_4SQ)_3$ in polar solvents, followed by the ligand exchange reaction of the LBMV tautomer, $[Cr^{III}(X_4BQ)(X_4SQ)(X_4Cat)]$, by the solvent molecules or the chelate reagents. Their structural and spectroscopic results could lead to further progress in the understanding of systems with comparisons to the tris-type LBMV complexes, $[Cr^{III}(X_4SQ)_{3-n}(X_4Cat)_n]^{n-}$.[6]

Acknowledgment. The authors acknowledge financial support by a Grant-in-Aid for Scientific Research (Priority Area No. 10149101) from The Ministry of Education, Science, Sports and Culture of Japan.

Supporting Information Available: Crystal and structure refinement data, positional parameters, anisotropic displacement parameters, and complete listings of bond distances and angles of **1**, **3**, and **5**, in CIF format. This material is available free of charge via the Internet at http://pubs.acs.org.

IC025643P